First Principle Calculation of Cohesive Energy of Xenon Segregated Grain Boundary of UO_2

Jae Joon Kim [a], Hyun Woo Seong,[a] Ho Jin Ryu [a*]
[a]*Department of Nuclear and Quantum Engineering, KAIST, Daejeon 34141, Republic of Korea*
[*]*Corresponding author: hojinryu@kaist.ac.kr*

1. Introduction

Grain boundaries are the most common structural defects in UO_2 nuclear fuels and play an important role in accommodation of fission products, which serve as nucleation sites for fission gas bubbles metallic and oxide precipitates. Some of the fission products formed during normal operation are deposited at the UO_2 grain boundary. Hocking et al. gave the segregation tendency and the form of segregation of 32 different fission products in UO_2 fuel. [1] Among them, xenon is element which exist in high concentrations in irradiated nuclear fuel and which have high tendency to segregate.

DFT is actively used to calculate material properties such as formation energy, phonon calculation, and density of state. Many groups have already conducted studies on grain boundary segregation and cohesive energy of materials using DFT calculations. [2-4] DFT analysis also has been used investigate the behavior of fission products inside nuclear fuel lattice. [5,6] In our previous research, the effect of segregation of fission products on UO_2 grain boundary cohesive energy was analyzed by DFT calculations. [7] It was confirmed that xenon segregates well in the site with the largest free volume of the Σ3(111)/[110] UO_2 grain boundary and segregated xenon effectively reduces the grain boundary cohesive energy by DFT calculations.

In this study, the cohesive energy change according to the concentration of xenon on the grain boundary was calculated by DFT. Not only Σ3(111)/[110] grain boundary but also Σ9(221)/[110] grain boundaries were used for calculation. These two grain boundaries were selected for calculation because they are the CSL grain boundaries with the highest frequency of existence in UO_2. [8] The calculated grain boundary cohesive energy can be used to derive the values such as strength, fracture toughness, and threshold pressure for grain boundary separation by intergranular bubble of high burnup nuclear fuel, and will contribute to the safety analysis of nuclear reactor.

2. Methods and Results

2.1 Computational details.

Total energy calculations by DFT were performed with the projector-argument-wave method as implemented in the Vienna *ab inito* simulation package (VASP). [9] The generalized gradient approximation (GGA) with Perdew-Burke-Ernzerhof (PBE) was used for exchange correlation functional, and the projected augmented wave (PAW) method were used to substitute core electrons of uranium, oxygen, and fission products atoms. [10-12] The Hubbard *U* correction is used to describe strongly correlated electrons in 5*f* orbital in uranium atoms. For value of U_{eff}, 3.96 eV was chosen for all conducted calculations in this study. This value is very close to the value used by Dudarev et al. [13] A plane wave basis set with a cut off energy of 500 eV was used. Spin polarization was considered in all calculations. Convergence of the electronic relaxation was satisfied when the total energy change was smaller than 10^{-7} eV/atom. Structural relaxation was conducted with conjugate-gradient algorithm until the Hellmann-Feynman force are less than 0.02 eV/Å.

2.2 Grain boundary segregation energy of xenon in UO_2 calculation

Σ3(111)/[110], Σ9(221)/[110] UO_2 grain boundary structures and segregation sites are depicted in Figure 1. Σ3(111)/[110] grain boundary consists of 120 atoms and has a tilt angle of 109.47°. Σ9(221)/[110] grain boundary has 102 atoms and tilt angle of 141.06°. The grain boundary segregation energy was calculated according to equation (1) below.

$$E_{seg/X} = E_{GB/X} - E_{GB/ref} \quad (1)$$

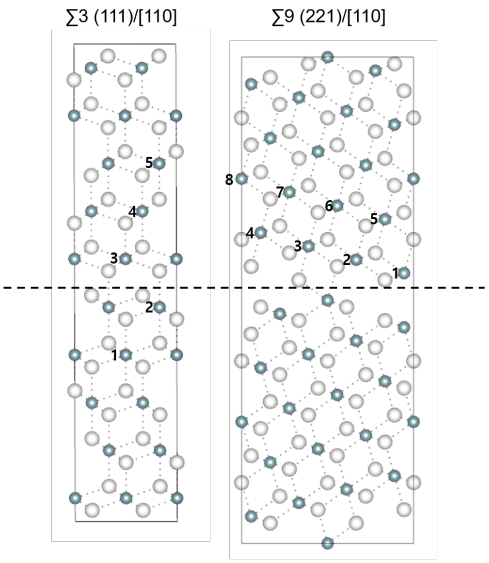

Figure 1. Grain boundary structures and segregation sites used in DFT calculation.

$E_{seg/X}$ is the grain boundary segregation energy at site X, $E_{GB/X}$ is the total energy calculated by VASP at site X, and $E_{GB/ref}$ is the total energy calculated by VASP at the reference site. The reference site was determined to be site 5 in the case of Σ3(111)/[110] and site 8 in the case of Σ9(221)/[110], and the selection criterion was the site farthest from the grain boundary. The segregation energy of xenon for the two grain boundaries is depicted in Figure 2. The site with the largest free volume in the grain boundary showed the most stable appearance.

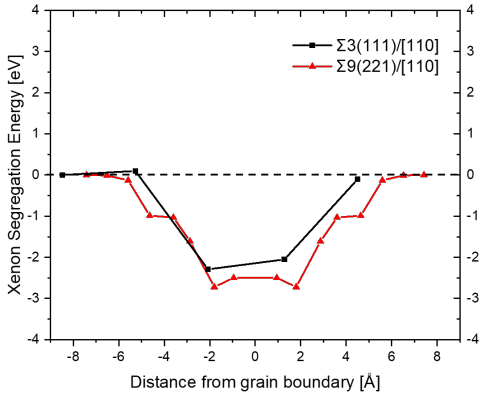

Figure 2. Grain boundary segregation energy of xenon.

The grain boundary cohesive energy was calculated by comparing the total energy before and after separation by adding a gap of 15 angstroms between grain boundaries based on the segregation structure at the site where xenon is most stable and divided by grain boundary area according to equation (2).

$$E_{coh/X} = (E_{seperated\ GB/X} - E_{GB/X})/A_{GB} \quad (2)$$

$E_{coh/X}$ is the grain boundary cohesive energy, $E_{seperated\ GB/X}$ is the total energy after grain boundary separation, and A_{GB} is the grain boundary area. A z-axis view of the grain boundaries used to calculate the cohesive energy is depicted in Figure 3. Figure 4 shows the grain boundary cohesive energy according to the area concentration of xenon. In both grain boundaries, when the area concentration of xenon increases, the grain boundary cohesive energy decreases. This means that the higher the concentration of xenon in the UO_2 grain boundary, the weaker the adhesion of the grain boundary. According to the exponential trend line, at the Σ3(111)/[110] grain boundary, the grain boundary cohesive energy becomes 0 J/m^2 when the area concentration of xenon is about 0.013 xenon/Å^2. In the case of the Σ9(221)/[110] grain boundary, when the area concentration of xenon is about 0.015 xenon/Å^2, grain boundary cohesive energy becomes 0 J/m^2

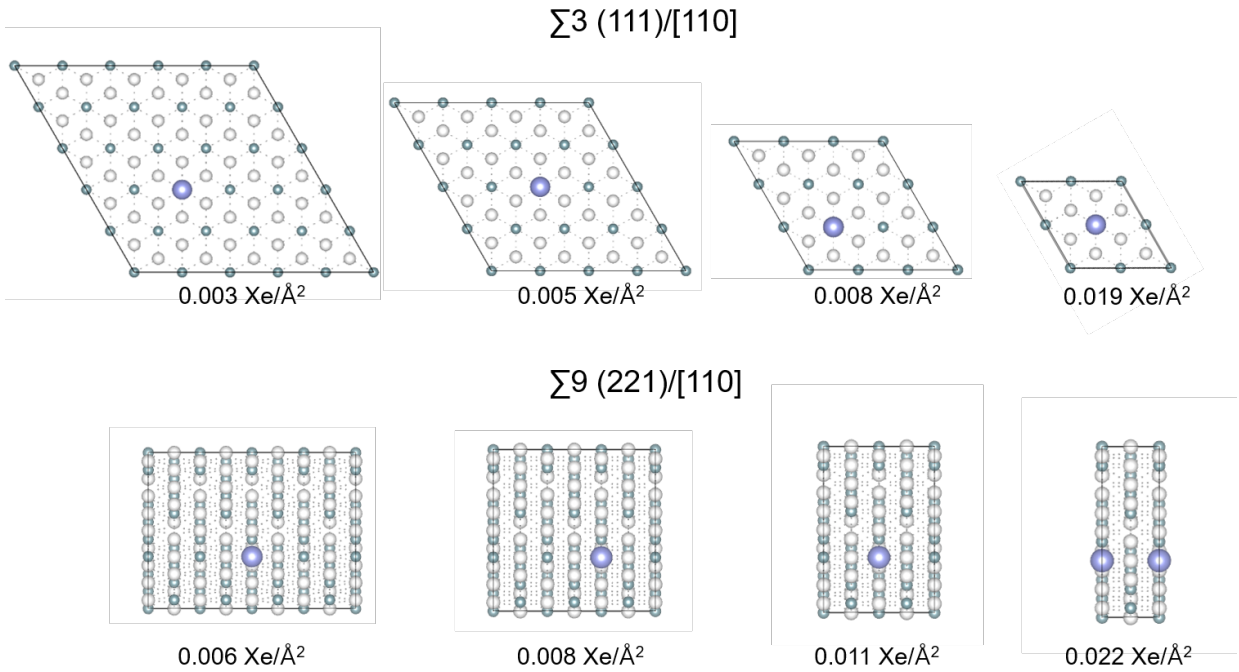

Figure 3. Z-axis view of grain boundaries used in cohesive energy calculations according to xenon concentration.

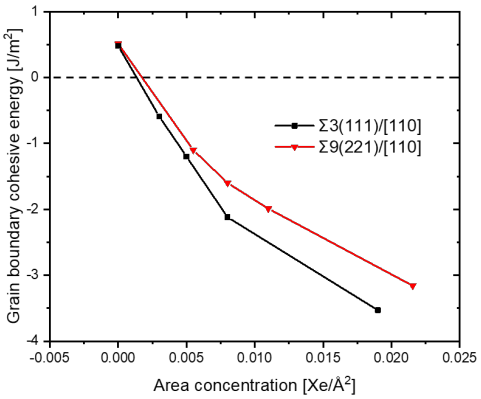

Figure 4. Grain boundary cohesive energy of xenon segregated UO_2 grain boundary along the area concentration of xenon.

From this calculation, the concentration of xenon on the grain boundary of UO2 causing fuel fragmentation is determined. The results of this study can be used to make a model of the nuclear fuel pulverization phenomenon, and the development of the model can help in the safety analysis of a nuclear reactor in an accident situation.

Acknowledgments
This study is supported by the National Research Foundation, MIST, Republic of Korea (NRF-2022M2E9A304619011).

REFERENCES

[1] W.H. Hocking, A.M. Duclos, L.H. Johnson, Study of fission-product segregation in used CANDU fuel by X-ray photoelectron spectroscopy (XPS) II, J. Nucl. Mater. 209 (1994) 1–26. https://doi.org/10.1016/0022-3115(94)90243-7.

[2] Y.J. Hu, Y. Wang, W.Y. Wang, K.A. Darling, L.J. Kecskes, Z.K. Liu, Solute effects on the Σ3 111[11-0] tilt grain boundary in BCC Fe: Grain boundary segregation, stability, and embrittlement, Comput. Mater. Sci. (2020). https://doi.org/10.1016/j.commatsci.2019.109271.

[3] J. Li, C. Zhang, L. Xu, Z. Zhang, N. Dong, Y. Liu, J. Wang, Y. Zhang, L. Ling, P. Han, Effects of B on the segregation of Mo at the Fe-Cr-NiΣ5(210) grain boundary, Phys. B Condens. Matter. (2019). https://doi.org/10.1016/j.physb.2019.05.018.

[4] M. Yamaguchi, First-principles study on the grain boundary embrittlement of metals by solute segregation: Part I. iron (Fe)-solute (B, C, P, and S) systems, in: Metall. Mater. Trans. A Phys. Metall. Mater. Sci., 2011. https://doi.org/10.1007/s11661-010-0381-5.

[5] D.A. Andersson, B.P. Uberuaga, P. V. Nerikar, C. Unal, C.R. Stanek, U and Xe transport in UO2±x: Density functional theory calculations, Phys. Rev. B - Condens. Matter Mater. Phys. (2011). https://doi.org/10.1103/PhysRevB.84.054105.

[6] G. Brillant, F. Gupta, A. Pasturel, Investigation of molybdenum and caesium behaviour in urania by ab initio calculations, J. Phys. Condens. Matter. (2009). https://doi.org/10.1088/0953-8984/21/28/285602.

[7] J.J. Kim, H.W. Seong, H.J. Ryu, First principles calculations of cohesive energy of fission-product-segregated grain boundary of UO2, J. Nucl. Mater. 566 (2022) 153780. https://doi.org/10.1016/j.jnucmat.2022.153780.

[8] N.R. Williams, M. Molinari, S.C. Parker, M.T. Storr, Atomistic investigation of the structure and transport properties of tilt grain boundaries of UO2, J. Nucl. Mater. 458 (2015) 45–55. https://doi.org/10.1016/j.jnucmat.2014.11.120.

[9] G. Kresse, J. Furthmiiller, Efficiency of ab-initio total energy calculations for metals and semiconductors, Comput. Mater. Sci. (1996).

[10] J.P. Perdew, K. Burke, M. Ernzerhof, Generalized gradient approximation made simple, Phys. Rev. Lett. (1996). https://doi.org/10.1103/PhysRevLett.77.3865.

[11] J.P. Perdew, K. Burke, Comparison shopping for a gradient-corrected density functional, Int. J. Quantum Chem. (1996). https://doi.org/10.1002/(SICI)1097-461X(1996)57:3<309::AID-QUA4>3.0.CO;2-1.

[12] P.E. Blöchl, Projector augmented-wave method, Phys. Rev. B. (1994). https://doi.org/10.1103/PhysRevB.50.17953.

[13] M.R. Castell, S.L. Dudarev, C. Muggelberg, A.P. Sutton, G.A.D. Briggs, D.T. Goddard, Surface structure and bonding in the strongly correlated metal oxides NiO and UO2, J. Vac. Sci. Technol. A Vacuum, Surfaces, Film. (1998). https://doi.org/10.1116/1.581232.